

Bulk Heterojunction Solar Cells Using Thieno[3,4-*c*]pyrrole-4,6-dione and Dithieno[3,2-*b*:2',3'-*d*]silole Copolymer with a Power Conversion Efficiency of 7.3%

Ta-Ya Chu,[†] Jianping Lu,^{*,†} Serge Beaupré,[‡] Yanguang Zhang,[†] Jean-Rémi Pouliot,[‡] Salem Wakim,[†] Jiayun Zhou,[†] Mario Leclerc,^{*,‡} Zhao Li,[‡] Jianfu Ding,[‡] and Ye Tao^{*,†}

[†]Institute for Microstructural Sciences and [‡]Institute for Chemical Process and Environmental Technology, National Research Council of Canada, Ottawa, Ontario K1A 0R6, Canada

^{*}Département de Chimie, Université Laval, Quebec City, Quebec, G1V 0A6, Canada

 Supporting Information

ABSTRACT: A new alternating copolymer of dithienosilole and thienopyrrole-4,6-dione (PDTSTPD) possesses both a low optical bandgap (1.73 eV) and a deep highest occupied molecular orbital energy level (5.57 eV). The introduction of branched alkyl chains to the dithienosilole unit was found to be critical for the improvement of the polymer solubility. When blended with PC₇₁BM, PDTSTPD exhibited a power conversion efficiency of 7.3% on the photovoltaic devices with an active area of 1 cm².

Bulk heterojunction (BHJ) organic solar cells based on conjugated p-type polymers and n-type fullerene derivatives have been intensively investigated in both academia and industry over the past decade due to their potential of being fabricated on flexible and light-weight substrates using high-throughput printing techniques and providing low-cost solar electricity.¹ Significant progress has been made in this field, and the power conversion efficiencies (PCEs) of solution-processed polymer solar cells have reached 7–8%, primarily due to the development of new low-bandgap p-type materials² and better control of the nanoscale morphology of the interpenetrating electron donor/acceptor networks.³

After years of intensive interdisciplinary research, some basic rules have become clear for designing an efficient p-type material for solar cell applications.⁴ First, the material should possess a relatively low optical bandgap (1.2–1.9 eV) and have strong optical absorption in the solar spectral range. Second, the material should have a low-lying HOMO energy level to offer high open circuit voltage (*V*_{oc}) when blended with a fullerene derivative as the photovoltaic (PV) active layer. Third, the energy offset between the LUMO energy levels of the polymer and the fullerene derivative should be well controlled to be just large enough to provide a driving force for efficient charge separation and not cause too much energy loss. Fourth, the material should have good hole mobility for efficient charge transport. Finally, the material should have good solubility in organic solvents for solution processing.

Along these lines, the combination of electron-rich (*push*) and electron-deficient (*pull*) moieties has been used effectively to

lower the bandgap of alternating conjugated polymers. Recent studies show that such *push–pull* structures can also enhance charge carrier mobility due to the reduced interchain $\pi-\pi$ stacking distance.⁵ In this regard, a number of electron-rich units, such as 2,7-carbazole,⁶ indolo[3,2-*b*]carbazole,⁷ cyclopenta[2,1-*b*:3,4-*b'*]dithiophene,⁸ dithieno[3,2-*b*:2',3'-*d*]silole,⁹ and benzo[1,2-*b*:4,5-*b'*]dithiophene,¹⁰ and quite a few electron-deficient units, such as 2,1,3-benzothiadiazole,¹¹ diketopyrrolo[3,4-*c*]pyrrole-1,4-dione,¹² ester- or ketone-substituted thieno[3,4-*b*]thiophene,² and thieno[3,4-*c*]pyrrole-4,6-dione,¹³ have been developed. However, different combinations of *push–pull* structures can result in totally different optoelectronic properties.¹⁴ It is still challenging to achieve a low-bandgap polymer with a deep HOMO energy level while maintaining enough driving force for electron transfer to fullerenes in BHJ solar cells. On the other hand, although the design and use of side chains is a classic topic in organic synthesis, it has gained growing attention in the field of organic electronics since it affects not only the solubility but also the molecular packing and the interaction between the polymer and acceptor molecules.¹⁵ In this work, we demonstrate for the first time that a low bandgap (1.73 eV) and a deep HOMO energy level (5.57 eV) can be simultaneously obtained from an alternating copolymer of 4,4-bis(2-ethylhexyl)-dithieno[3,2-*b*:2',3'-*d*]silole and *N*-octylthieno[3,4-*c*]pyrrole-4,6-dione (PDTSTPD). The advantages of the dithienosilole unit over its carbon-bridged counterpart include better hole-transport properties and lower HOMO energy levels.¹⁶ With a rational choice of branched alkyl chains on the dithienosilole unit, the resulting polymer PDTSTPD has an excellent solubility in a wide range of organic solvents, including chloroform, chlorobenzene (CB), and dichlorobenzene (DCB), which is a critical material parameter for applications in large-scale device production. By blending PDTSTPD with [6,6]-phenyl C₇₁-butyric acid methyl ester (PC₇₁BM) at a weight ratio of 1:2 as the PV active material, a PCE of 7.3% has been achieved on solar cells with an active area of 1 cm² under simulated AM 1.5G solar irradiation of 100 mW/cm².

The alternating copolymer PDTSTPD was prepared by a Stille coupling reaction between 4,4-bis(2-ethylhexyl)-2,6-bis(trimethyltin)-dithieno[3,2-*b*:2',3'-*d*]silole and 1,3-dibromo-5-octylthieno[3,4-*c*]pyrrole-4,6-dione in refluxing

Received: January 12, 2011

Published: March 04, 2011

Scheme 1. Synthetic Route to an Alternating Copolymer, PDTSTPD

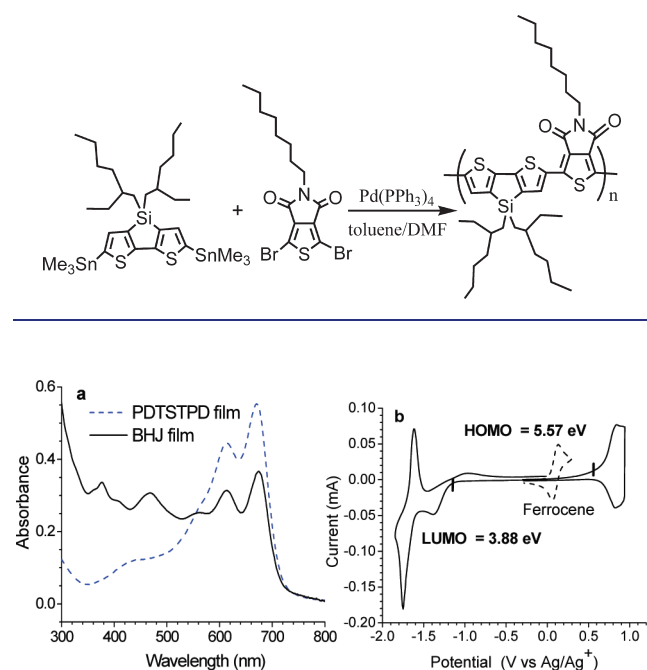


Figure 1. (a) UV-vis absorption spectra of neat PDTSTPD films (50 nm) and PDTSTPD/PC₇₁BM BHJ films (1:2 by weight, 90 nm). (b) Cyclic voltammogram of a PDTSTPD film cast on a platinum wire in Bu₄NBF₄/CH₃CN at a scan rate of 50 mV s⁻¹.

toluene/dimethylformamide (10:1) under Ar in the presence of Pd(PPh₃)₄ as the catalyst for 42 h, as shown in Scheme 1. Trimethylphenyltin (0.075 equiv) and bromobenzene (0.3 equiv) were then consecutively added at a time interval of 5 h to end-cap the polymer. The polymer was precipitated in methanol, collected by filtration, and purified by Soxhlet extraction. Low-molecular-weight oligomers were successfully removed by extraction with hexanes and dichloromethane. The remaining high-molecular-weight part was extracted with chloroform. The purified polymer has a number-average molecular weight of 28 kDa and a polydispersity index of 1.6, as determined by gel permeation chromatography using CB as the eluent. This high-molecular-weight polymer PDTSTPD could be readily dissolved in chlorinated solvents even at room temperature. In contrast, when the two ethylhexyl groups on the dithienosilole unit were replaced by two linear hexyl groups, the resulting polymer had a very poor solubility and precipitated out during polymerization, and the polymer molecular weight reached only 4.3 kDa as a result. Polymer PDTSTPD shows a glass transition temperature around 109 °C, as measured by differential scanning calorimetry. The hole mobility of PDTSTPD is about 1×10^{-4} cm²/(V·s), as measured from a bottom-contact field effect transistor on a SiO₂/Si substrate.

The PDTSTPD film spin-cast from CB solution has two strong absorption peaks at 614 and 670 nm, respectively. The onset of the optical absorption of the PDTSTPD film is at ~717 nm, corresponding to an optical bandgap of 1.73 eV, which is about 0.1 eV lower than that of the recently reported benzodithiophene/thienopyrrole-4,6-dione copolymer.¹³ As PDTSTPD has low absorption below 500 nm, PC₇₁BM was chosen as the electron acceptor for the BHJ solar cell in order to increase the

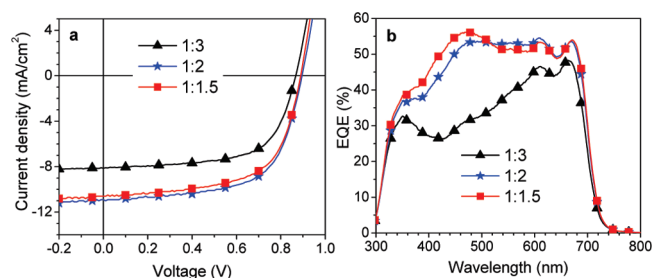


Figure 2. (a) *J*–*V* characteristics and (b) EQE curves of the solar cells based on the PDTSTPD/PC₇₁BM blends with different weight ratios fabricated from DCB solutions containing 3 vol % DIO.

light absorption between 300 and 550 nm. As can be seen from Figure 1a, the PDTSTPD/PC₇₁BM BHJ film (1:2 by weight) has strong absorption over a broad wavelength range, 300–690 nm. PDTSTPD exhibits reversible cathodic reduction and anodic oxidation curves in cyclic voltammetry measurements, as shown in Figure 1b. Based on the onset potentials of the oxidation and reduction processes, the HOMO and LUMO energy levels of PDTSTPD are estimated to be at 5.57 and 3.88 eV, respectively. The obtained electrochemical bandgap (1.69 eV) is in good agreement with the optically measured one (1.73 eV).

The PV performance of PDTSTPD was first investigated by blending PDTSTPD with PC₇₁BM in 1,2-DCB at different weight ratios. 1,8-Diiodooctane (DIO, 3% by volume) was added as a processing additive. The PV device structure employed in this study is ITO/PEDOT:PSS (30 nm)/PDTSTPD:PC₇₁BM (90 nm)/BCP (5 nm)/Al, where BCP stands for bathocuproine, which functions as a hole/exciton blocking layer.¹⁷ The processes for device fabrication and characterization are described in detail in the Supporting Information (SI). The devices were tested in air without encapsulation. Figure 2 shows the typical current density–voltage (*J*–*V*) characteristics under one sun of simulated AM 1.5G solar irradiation (100 mW/cm²) and the external quantum efficiency (EQE) spectra of PV devices with different PDTSTPD:PC₇₁BM weight ratios (1:1.5, 1:2, and 1:3). Among the devices prepared using DCB as the processing solvent, the best performance was obtained at a weight ratio of 1:2, with *V*_{oc} = 0.90 V, *J*_{sc} = 10.95 mA/cm², a fill factor (FF) of 0.63, and an overall PCE of 6.2%. One striking feature of PDTSTPD-based solar cells is the high *V*_{oc} resulting from the deep HOMO level of PDTSTPD. As expected, the devices exhibit a broad photore-sponse range from 350 to 690 nm, with a maximum EQE of 55% at 608 nm. The wavelength integration of the product of the EQE curve and the standard AM 1.5G solar spectrum yields a calculated *J*_{sc} of 10.54 mA/cm², within 4% error compared to the *J*_{sc} value obtained from the *J*–*V* measurement.

We found that the device performance can be further improved by changing the device fabrication solvent from DCB to CB containing 3% DIO by volume. The weight ratio of PDTSTPD to PC₇₁BM and the active layer thickness were kept at 1:2 and 90 nm, respectively. The best device, prepared using CB with 3% DIO, reached an EQE-calibrated PCE of 7.3%, with *V*_{oc} = 0.88 V, *J*_{sc} = 12.2 mA/cm², and FF = 0.68. The maximum EQE reaches 65% at 608 nm, compared with 55% for the devices spin-cast from DCB solutions. Figure 3 shows the typical current density–voltage (*J*–*V*) characteristics under simulated AM 1.5G solar irradiation (100 mW/cm²) and the EQE curve for the best device.

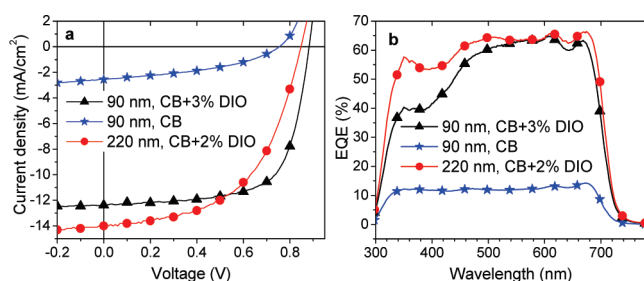


Figure 3. (a) J - V characteristics and (b) EQE curves of the solar cells based on the 1:2 PDTSTPD/PC₇₁BM blend with different thicknesses fabricated from CB solutions (with no additive and 2 or 3 vol % DIO).

It is important to point out that the processing additive, DIO, played an important role in improving the nanoscale morphology of the BHJ film. Without this additive, the device performance dropped significantly, with a PCE below 1.0%. Study of the film morphology by atomic force microscopy (AFM) showed that PC₇₁BM formed large isolated domains ($\sim 0.4 \mu\text{m}$ diameter) in the blend film prepared without using DIO (see SI Figure S5). These large isolated domains are not favorable for efficient exciton dissociation and charge transport. As a result, the J_{sc} dropped from 12.2 to 2.6 mA/cm², and the V_{oc} and FF also decreased significantly. When DIO (3% by volume) was added to the solution, the resulting BHJ film showed a much more uniform and finer domain structure with an average domain size of 20–40 nm, ideal for an effective polymer/PC₇₁BM interpenetrating network (Figure S5). As a result, the device performance was greatly improved. This finding highlights the importance of morphology control toward high-performance solar cells.

We also tested PDTSTPD/PC₇₁BM-based devices with thicker active layers. A PV device with an active layer of 220 nm and an area of 1.0 cm² reached an EQE-calibrated PCE of 6.1%, with $J_{\text{sc}} = 13.3 \text{ mA/cm}^2$, $V_{\text{oc}} = 0.85 \text{ V}$, and FF = 0.54, as shown in Figure 3. This preliminary result demonstrates the potential of PDTSTPD for use in thick-active-layer solar cells ($d > 200 \text{ nm}$). We believe that a higher efficiency can be expected after device optimization. A thicker active layer will not only give us access to the second, stronger light absorption maximum as calculated from optical simulation,¹⁸ but will also make it possible to fabricate PV devices by roll-to-roll printing techniques.

In conclusion, a new alternating copolymer of dithienosilole and thienopyrrole-4,6-dione, PDTSTPD, has been designed and synthesized. Four unique features of PDTSTPD—a low bandgap (1.73 eV), a deep HOMO level (5.57 eV), an excellent solubility in organic solvents even at room temperature, and a relatively simple synthetic procedure—make this material a very promising candidate for solar cell applications. A high power conversion efficiency of 7.3% has been obtained on PV devices with an active area of 1.0 cm². We fully expect that the device performance can be further improved by the optimization of the material and the device fabrication.

■ ASSOCIATED CONTENT

Supporting Information. Experimental details of polymers synthesis, instruments, AFM images of the polymer/PC₇₁BM blends, device fabrication, and characterization. This material is available free of charge via the Internet at <http://pubs.acs.org>.

■ AUTHOR INFORMATION

Corresponding Author

jianping.lu@nrc.ca; mario.leclerc@chm.ulaval.ca; ye.tao@nrc.ca

■ ACKNOWLEDGMENT

This work was financially supported by Sustainable Development Technology Canada (SDTC). The authors thank Dr. Y. Zou from Université Laval and Mr. E. Estwick, Mr. H. Fukutani, Mr. G. Robertson, Dr. S. Alem, and Dr. S. Tsang at NRC for their technical support, and Drs. R. Gaudiana, D. Waller, and G. Dennler of Konarka Technologies for very helpful discussions.

■ REFERENCES

- (1) (a) Gunes, S.; Neugebauer, H.; Sariciftci, N. S. *Chem. Rev.* **2007**, *107*, 1324–1338. (b) Krebs, F. C. *Sol. Energy Mater. Sol. Cells* **2009**, *93*, 394–412. (c) Krebs, F. C. *Sol. Energy Mater. Sol. Cells* **2009**, *93*, 465–475. (d) Hoppe, H.; Sariciftci, N. S. *J. Mater. Chem.* **2006**, *16*, 45–61. (e) Dennler, G.; Scharber, M. C.; Brabec, C. J. *Adv. Mater.* **2009**, *21*, 1323–1338. (f) Brabec, C. J.; Gowrisanker, S.; Halls, J. J. M.; Laird, D.; Jia, S.; Williams, S. P. *Adv. Mater.* **2010**, *22*, 3839–3856.
- (2) (a) Liang, Y.; Xu, Z.; Xia, J.; Tsai, S.; Wu, Y.; Li, G.; Ray, C.; Yu, L. *Adv. Mater.* **2010**, *22*, E135–E138. (b) Chen, H. Y.; Hou, J.; Zhang, S.; Liang, Y.; Yang, G.; Yang, Y.; Yu, L.; Wu, Y.; Li, G. *Nature Photon.* **2009**, *3*, 649–653.
- (3) (a) Peet, J.; Kim, J. Y.; Coates, N. E.; Ma, W. L.; Moses, D.; Heeger, A. J.; Bazan, G. C. *Nat. Mater.* **2007**, *6*, 497–500. (b) Lee, J. K.; Ma, W. L.; Brabec, C. J.; Yuen, J.; Moon, J. S.; Kim, J. Y.; Lee, K.; Bazan, G. C.; Heeger, A. J. *J. Am. Chem. Soc.* **2008**, *130*, 3619–3623. (c) Hoven, C. V.; Dang, X. D.; Coffin, R. C.; Peet, J.; Nguyen, T. Q.; Bazan, G. C. *Adv. Mater.* **2010**, *22*, E63–E66. (d) Ma, W.; Yang, C.; Gong, X.; Lee, K.; Heeger, A. J. *Adv. Funct. Mater.* **2005**, *15*, 1617–1622. (e) Li, G.; Shrotriya, V.; Huang, J.; Yao, Y.; Moriarty, T.; Emery, K.; Yang, Y. *Nat. Mater.* **2005**, *4*, 864–868.
- (4) Scharber, M. C.; Mühlbacher, D.; Koppe, M.; Denk, P.; Waldauf, C.; Heeger, A. J.; Brabec, C. J. *Adv. Mater.* **2006**, *18*, 789–794.
- (5) (a) Bürgi, L.; Turbiez, M.; Pfeiffer, R.; Bilenewald, F.; Kirner, H.; Winnewisser, C. *Adv. Mater.* **2008**, *20*, 2217–2224. (b) Li, Y.; Singh, S. P.; Sonar, P. *Adv. Mater.* **2010**, *22*, 4862–4866. (c) Tsao, H. N.; Cho, D. M.; Park, I.; Hansen, M. R.; Mavrinskiy, A.; Yoon, D. Y.; Graf, R.; Pisula, W.; Spiess, H.; Müllen, K. *J. Am. Chem. Soc.* **2011**, *133*, 2605–2612.
- (6) (a) Blouin, N.; Michaud, A.; Leclerc, M. *Adv. Mater.* **2007**, *19*, 2295–2300. (b) Park, S. H.; Roy, A.; Beaupré, S.; Cho, S.; Coates, N.; Moon, J. S.; Moses, D.; Leclerc, M.; Lee, K.; Heeger, A. J. *Nature Photon.* **2009**, *3*, 297–302.
- (7) Lu, J.; Liang, F.; Drolet, N.; Ding, J.; Tao, Y.; Movileanu, R. *Chem. Commun.* **2008**, 5315–5317.
- (8) (a) Zhu, Z.; Waller, D.; Gaudiana, R.; Morana, M.; Mühlbacher, D.; Scharber, M. C.; Brabec, C. *Macromolecules* **2007**, *40*, 1981–1986. (b) Mühlbacher, D.; Scharber, M.; Morana, M.; Zhu, Z.; Waller, D.; Gaudiana, R.; Brabec, C. *Adv. Mater.* **2006**, *18*, 2884–2889.
- (9) (a) Liao, L.; Dai, L.; Smith, A.; Durstock, M.; Lu, J.; Ding, J.; Tao, Y. *Macromolecules* **2007**, *40*, 9406–9412. (b) Hou, J.; Chen, H.; Zhang, S.; Li, G.; Yang, Y. *J. Am. Chem. Soc.* **2008**, *130*, 16144–16145.
- (10) Pan, H.; Li, Y.; Wu, Y.; Liu, P.; Ong, B.; Zhy, S.; Xu, G. *Chem. Mater.* **2006**, *18*, 3237–3241.
- (11) Zhang, F.; Jespersen, K. G.; Björström, C.; Svensson, M.; Andersson, M. R.; Sundström, V.; Magnusson, K.; Moons, E.; Yartsev, A.; Inganäs, O. *Adv. Funct. Mater.* **2006**, *16*, 667–674.
- (12) Wienk, M. M.; Turbiez, M.; Gilot, J.; Janssen, R. A. J. *Adv. Mater.* **2008**, *20*, 2556–2560.
- (13) (a) Zou, Y.; Najari, A.; Berrouard, P.; Beaupré, S.; Aich, B.; Tao, Y.; Leclerc, M. *J. Am. Chem. Soc.* **2010**, *132*, 5330–5331. (b) Piliago, C.;

Holcombe, T. W.; Douglas, J.; Woo, C. H.; Beaujuge, P. M.; Fréchet, J. M. J. *J. Am. Chem. Soc.* **2010**, *132*, 7595–7597.

(14) Zhou, E.; Cong, J.; Tajima, K.; Hashimoto, K. *Chem. Mater.* **2010**, *22*, 4890–4895.

(15) (a) Liang, Y.; Feng, D.; Wu, Y.; Tsai, S. T.; Li, G.; Ray, C.; Yu, L. *J. Am. Chem. Soc.* **2009**, *131*, 7792–7799. (b) Johns, J. E.; Muller, E. A.; Frechet, J. M. J.; Harris, C. B. *J. Am. Chem. Soc.* **2010**, *132*, 15720–15725.

(16) Chen, H. Y.; Hou, J.; Hayden, A. E.; Yang, H.; Houk, K. N.; Yang, Y. *Adv. Mater.* **2010**, *22*, 371–375.

(17) Peumans, P.; Bulovic, V.; Forrest, S. R. *Appl. Phys. Lett.* **2000**, *76*, 2650–2652.

(18) Chu, T.; Alem, S.; Verly, P. G.; Wakim, S.; Lu, J.; Tao, Y.; Beaupré, S.; Leclerc, M.; Bélanger, F.; Désilets, D.; Rodman, S.; Waller, D.; Gaudiana, R. *Appl. Phys. Lett.* **2009**, *95*, 063304.